colour image processing, impulsive noise removal, colour image enhancement

Bogdan SMOLKA*

ON THE ADAPTIVE IMPULSIVE NOISE REMOVAL IN COLOR IMAGES

In this paper a novel adaptive filtering scheme for impulsive noise removal in colour images is presented. The noise detection algorithm is based on the concept of aggregated distances assigned to the pixels belonging to the filtering window. The value of the difference between the accumulated distance assigned to the central sample and to the pixel with the lowest rank, serves as an indicator of the presence of impulses injected into the image by the noise process. The output of the proposed filter is a weighted mean of the central pixel of the filtering window and the vector median of its samples. The obtained results show that the proposed filter outperforms existing impulse noise removal techniques for low noise contamination and can be used in various applications in which the detail preserving reduction of impulses play an important role.

1. INTRODUCTION

Computer vision systems very often use color information to sense the environment and therefore the correct processing of color information is of great importance in various tasks of pattern recognition and image understanding. Unfortunately, noise and other impairments associated with the acquisition and transmission can significantly degrade the value of the color information carried by digital images. It comes therefore as no surprise that the most common signal processing task is noise filtering. The reduction of noise is an essential part of any image processing based system, whether the final information is used for human perception or for an automatic inspection and analysis [1].

During image formation, acquisition, storage and transmission many types of distortions limit the quality of digital images. Transmission errors, periodic or random motion of the camera system during exposure, electronic instability of the image signal, electromagnetic interferences, sensor malfunctions, optic imperfections or aging of the storage material, all disturb the image quality. In many practical situations, images are corrupted by the so called *impulsive noise* caused mainly either by faulty image sensors or due to transmission errors resulting from man-made phenomena such as ignition transients in the vicinity of the receivers or even natural phenomena such as lightning in the atmosphere.

In this paper the problem of impulsive noise removal in color images is addressed and an efficient adaptive technique capable of removing the impulsive noise and preserving important image features is proposed. The paper is organized as follows. In the next section a short overview of the basic multichannel filtering schemes is provided. Then, the new filtering approach is described and its similarity to existing filtering schemes is discussed. Section 3 presents the construction of the new adaptive filtering scheme and section 4 covers the experimental results performed on test images contaminated with impulsive noise. The paper ends with a short conclusion.

2. VECTOR MEDIAN BASED FILTERS

A multichannel image is a mapping $\mathbb{Z}^2 \rightarrow \mathbb{Z}^m$ representing a two-dimensional matrix of size $N_1 \times N_2$ consisting of $m-$component samples (pixels), $\mathbf{x}_i = (x_{i1}, x_{i2}, \ldots, x_{im}) \in \mathbb{Z}^2$, where m denotes the number of channels, (in the case of standard color images, m equals 3). Components x_{ik}, for $k = 1, \ldots, m$ and $i = 1, 2, \ldots, N$, where $N = N_1 \cdot N_2$ denotes the number of image pixels, represent the color channel values quantified into the integer domain.

The majority of the nonlinear, multichannel filters intended for the suppression of impulse noise in color images are based on the ordering of vectors in a sliding filter window. The output of these filters is defined as the lowest ranked vector according to a specific vector ordering technique [2, 3].

Let the color images be represented in the commonly used RGB space and let $\{\mathbf{x}_1, \mathbf{x}_2, \ldots, \mathbf{x}_n\}$ be 3-dimensional vectors from the sliding filter window W, with $\mathbf{x}_1$ being the central element in W. The goal of the vector ordering is to arrange the set of n vectors $\{\mathbf{x}_1, \mathbf{x}_2, \ldots, \mathbf{x}_n\}$ belonging to W using some sorting criterion.

The most widely used ordering scheme is based on the aggregated distances assigned to the samples of W defined as $r_i = \sum_{j=1}^{n} \rho(\mathbf{x}_i, \mathbf{x}_j)$, where $\rho(\mathbf{x}_i, \mathbf{x}_j)$ is the distance between the $\mathbf{x}_i$ and $\mathbf{x}_j$. The increasing ordering of the quantities

* Silesian University of Technology, Dept. of Automatic Control, Akademicka 16, 44-100 Gliwice, Poland.
This work has been supported by the Polish Ministry of Science and Higher Education under R&D grant no. N N516374736 from the Science Budget 2009-2011.

$\{r_{(1)}, r_{(2)}, \ldots, r_{(n)}\}$, where $r_{(k)}$ denotes the $k-\text{th}$ aggregated distance, generates the ordered set of vectors $\{\mathbf{x}_{(1)}, \mathbf{x}_{(2)}, \ldots, \mathbf{x}_{(n)}\}$.

One of the most important noise reduction techniques is the *Vector Median Filter* (VMF), whose output is the vector $\mathbf{x}_{(1)}$ from W, for which the sum of distances to all other vectors belonging to W is minimized, (Fig. 1). The VMF is very efficient at reducing the impulses, preserves sharp edges and linear trends, however it does not preserve fine image structures, which are treated as noise and therefore generally the VMF tends to produce blurry images.

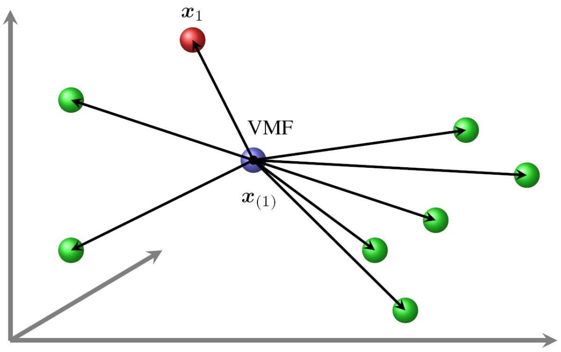

Fig. 1. The VMF output is the vector $\mathbf{x}_{(1)}$.

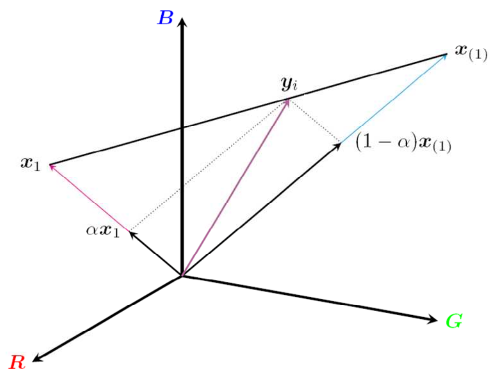

Fig. 2. Construction of the filter output as a weighted mean of the central pixel $\mathbf{x}_1$ and vector median $\mathbf{x}_{(1)}$.

The drawback of the filtering methods based on the ordering of samples according to the values of the aggregated distances is that the derived filters operate uniformly over the image and unnecessary replace pixels, which were not corrupted by the noise process.

To alleviate this drawback many switching mechanisms were introduced into the structure of the impulsive noise reduction filters [4,5]. The goal of a switching filtering scheme is to efficiently detect the noisy pixels and to replace them by a noise removal filter output, while preserving the uncorrupted samples.

3. PROPOSED FILTERING DESIGN

The well known local statistic filters constitute a class of linear minimum mean squared error estimators and they make use of the local mean and variance of the input set $W = \{x_1, x_2, \ldots, x_n\}$ defining the filter output for the gray-scale images as [6,7]

$$y_i = \hat{x}_i + \alpha\left(x_i - \hat{x}_i\right) = \alpha x_i + (1-\alpha)\hat{x}_i, \tag{1}$$

where $\hat{x}_i$ is the arithmetic mean of the image pixels belonging to the filtering window W centered at a pixel position i and α is a filter parameter estimated from the noisy image. Equation (1) can be rewritten using the notation $x_i = x_1$, as

$$y_1 = \alpha x_i + (1-\alpha)\hat{x}_i = \alpha x_1 + (1-\alpha)\hat{x}_1 = (1-\alpha)\left(\psi_1 x_1 + x_2 + \ldots + x_n\right)/n, \tag{2}$$

with $\psi_1 = (1-\alpha+n\alpha)/(1-\alpha)$ and the local statistic filter defined by (1) is reduced to the *central weighted average*, with a weighting coefficient ψ_1. In this way the set of weights $\{\psi_1, 1, 1, \ldots, 1\}$ is assigned to the set of pixels in the filtering window $\{x_1, x_2, \ldots, x_n\}$.

If the weighting is applied to the ordered sequence of gray-scale samples belonging to W: $\{x_{(1)}, \ldots, x_{(\mu)}, \ldots, x_{(n)}\}$, where $x_{(1)}$ and $x_{(n)}$ are the minimal and maximal pixel values and $x_{(\mu)}$, $(\mu = (n+1)/2)$ denotes the median of the input set, then $y_1 = \left(\sum_{k=1}^{n} \psi_k\right)^{-1} \sum_{k=1}^{n} \psi_k x_{(k)}$.

Taking the weighting set $\{1, 1, \ldots, \psi_\mu, \ldots, 1\}$, special emphasis is given to the median of the input set $x_{(\mu)}$. Hence

$$y_1 = \left(\frac{n}{n+\psi_\mu -1} \right) \hat{x}_1 + \left(\frac{\psi_\mu -1}{n+\psi_\mu -1} \right) x_{(\mu)} = (1-\alpha)\hat{x}_1 + \alpha x_{(\mu)}, \tag{3}$$

which is a compromise between the median $x_{(\mu)}$ and the average $\hat{x}_1$ controlled again by the parameter α.

Let us now apply a weighting structure defined by the weights $\{1, 0, \ldots, \psi_\mu, \ldots, 0\}$. Such a setting of the weights leads to the output defined by

$$y_1 = \frac{1}{1+\psi_\mu} \left(x_1 + \psi_\mu x_{(\mu)} \right) = \alpha x_1 + (1-\alpha) x_{(\mu)}. \tag{4}$$

If we work on the set of ordered vectors $\{\mathbf{x}_{(1)}, \mathbf{x}_{(2)}, \ldots, \mathbf{x}_{(n)}\}$ then (4) can be rewritten as

$$\mathbf{y}_1 = \frac{1}{1+\psi_1} \left(\mathbf{x}_1 + \psi_1 \mathbf{x}_{(1)} \right) = \alpha \mathbf{x}_1 + (1-\alpha) \mathbf{x}_{(1)}, \tag{5}$$

where the weighting set is defined as: $\{\psi_1, 0, \ldots, 0, 1, 0, \ldots, 0\}$ in which the weight ψ_1 is assigned to the *vector median* $\mathbf{x}_{(1)}$ of the input set from W and 1 is assigned to pixel $\mathbf{x}_1$.

Clearly, the filtering structure defined by (3) is similar to approach defined by (1), however, as our aim is to construct a filter capable of removing impulsive noise, instead of the mean value, the VMF output is used and the noise intensity estimation mechanism is regulated by the coefficient α, (Fig 2). In this way, the proposed technique is a compromise between the VMF and the identity operation. When an impulse is present, then the value of α should be 0, otherwise it should be 1.

The filtering efficiency of the proposed scheme depends strongly on the accuracy of the impulse detection. The straightforward choice would be to detect the impulses by measuring the difference between the central pixel of the filtering window and the vector median of its samples. However, such an approach is not suitable for noise detection, as the image texture and edges can be easily treated as noise, which leads to an extensive image smoothing, caused by unnecessary pixel replacement by the vector median.

The proposed switching filter is based on the difference between the aggregated distance r_1 assigned to the central pixel of the filtering window and the value of $r_{(1)}$ corresponding to the vector median output. Introducing the notation: $r_1 = r_c$ and $r_{(1)} = r_m$, the measure of pixel distortion r_d is then expressed as: $r_d = r_c - r_m$.

Figure 3 shows an example of the detected noise using a part of the test image LENA. The visual comparison of the noise map composed of the values of r_d and the differences between the noisy and original test image confirms the good noise detection ability of the proposed approach. The map of the detected noise corresponds very well with the real corruption derived from the noisy and clean images.

To discriminate between pixels corrupted by impulse noise and the undisturbed samples, a global thresholding scheme could be applied. However, the thresholding of the noise map would lead to many errors which would result in retaining the impulses and unnecessary undisturbed pixel replacement. To alleviate the problems connected with hard thresholding, a soft scheme has been applied. Utilizing the filtering framework expressed by Eq. (5), we can use the noise map as a distortion measure and make the α coefficient dependent on the values of the noise intensity r_d. In this way, every pixel will be replaced by the weighted mean of the central pixel of W and its vector median.

Of course, the efficiency of such a scheme depends heavily on the proper choice of the α coefficient. Experimental results indicates that satisfactory results can be achieved using various kernel functions known from the nonparametric estimation theory. Therefere, for the presentation of the filter efficiency the following form of the α coefficient has been chosen: $\alpha = \exp\left\{ -\left(r_d / h \right)^2 \right\}$, where h is a normalization parameter.

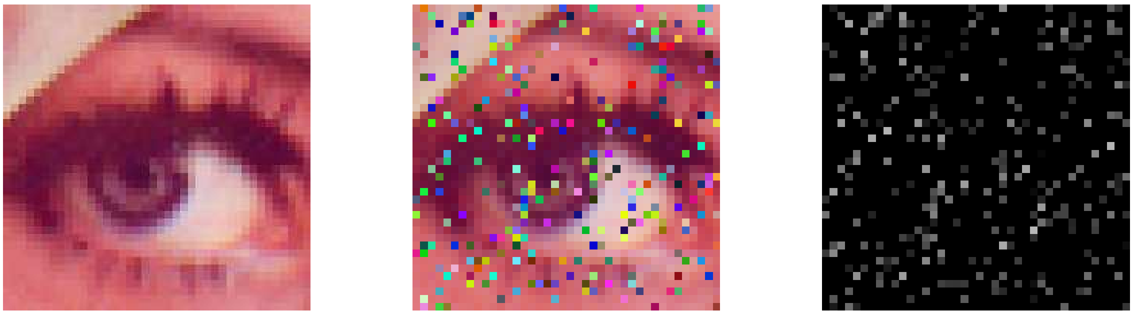

(a) original image (b) noisy image (c) real contamination

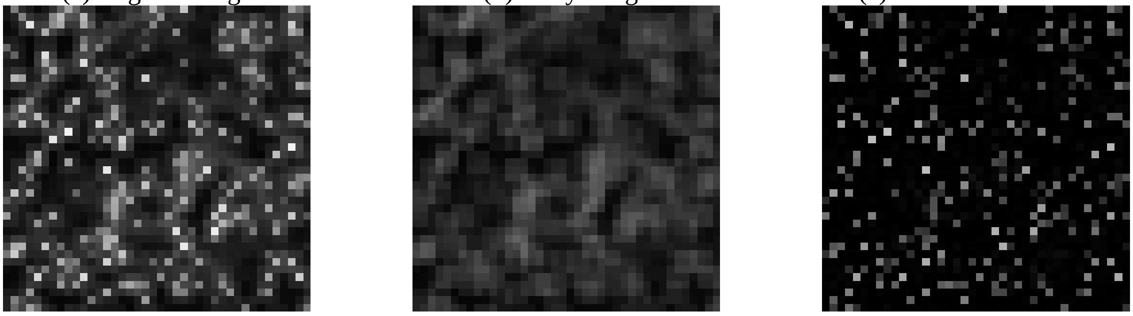

(d) map of r_c (e) map of r_m (f) detected noise: $r_c - r_m$

Fig. 3. Illustration of the noise detection scheme: test image (a), noisy image (b), injected impulse noise noise (c). Below the maps of r_c , r_m and their difference $r_d = r_c - r_m$ is presented (d-f)

4. EXPERIMENTS

In order to evaluate the effectiveness of the novel switching filter a set of test images (Fig. 4) was contaminated with three kinds of impulsive noise. In the first two noise models, the noisy pixels $\mathbf{x}_i = \{x_{i1}, x_{i2}, x_{i3}\}$ are defined as $x_{iq} = \rho_{iq}$ with probability π, and o_{iq} with probability $1-\pi$, where o_{iq} denotes the q -th component of the original pixel at position i and the contamination component ρ_{iq} is a random variable.

If the variable ρ can take any discrete value in the range $[0, 255]$ the uniform or random-valued impulsive noise model is obtained, which will be denoted in this paper as NM1, (this kind of noise was used to contaminate the test images presented in Fig. 3). If ρ takes only the value 0 or 255, the salt & pepper or fixed-valued impulse noise is modeled and it will be denoted as NM2. The third kind of noise denoted as NM3 is defined as $\mathbf{x}_i = \mathbf{o}_i$ with probability $(1-p)$, $\{\rho_{i1}, o_{i_2}, o_{i_3}\}$ with probability $p_1 \cdot p$, $\{o_{i_1}, \rho_{i2}, o_{i_3}\}$ with probability $p_2 \cdot p$, $\{o_{i_1}, \rho_{i2}, o_{i_3}\}$ with probability $p_3 \cdot p$ and $\{\rho_{i4}, \rho_{i4}, \rho_{i4}\}$ with probability $p_4 \cdot p$, [1, 8], where p is the noise intensity and $p_1, \ldots, p_4$ are corruption probabilities of each color channel, so that $\sum_1^4 p_\kappa = 1$. The variables $\rho_{i\kappa}$, $\kappa = 1, \ldots, 4$ take on the value 0 or 255 with equal probability and $p_\kappa = 0.25$ for $\kappa = 1, \ldots, 4$.

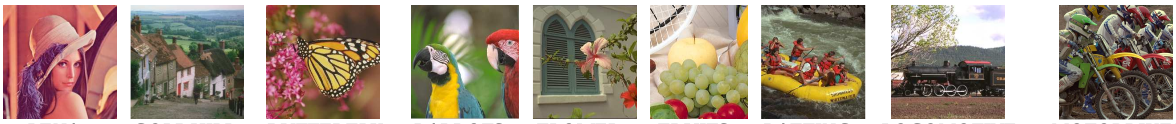

LENA *GOLDHILL* *BUTTERFLY* *PARROTS* *FLOWER* *FRUITS* *RAFTING* *LOCOMOTIVE* *MOTORBIKES*

Fig. 4. Test images used for the simulations

For the measurement of the restoration quality, the commonly *Peak Signal to Noise Ratio* (PSNR) was used and for the evaluation of the detail preservation capabilities of the proposed filtering design the *Mean Absolute Error* (MAE) has been utilized.

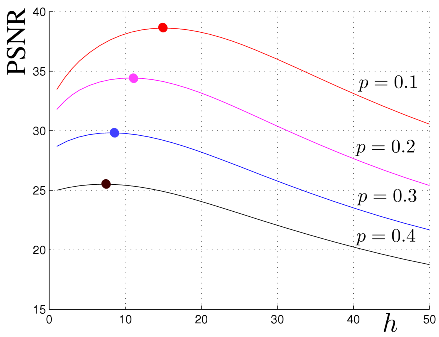

Fig. 5. Dependence of the PSNR on the h parameter for the LENA test image. The dots show the maxima of the plots and indicate the optimal h values.

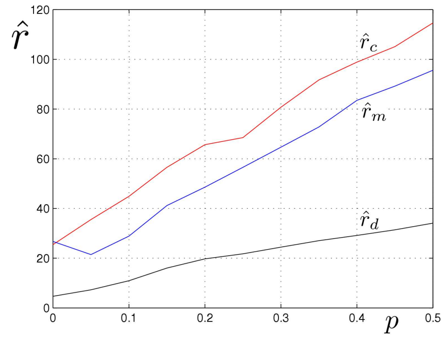

Fig. 6. Dependence of the mean values of r_m, r_c and r_d on the noise intensity p for the LENA image.

Figure 5 shows the dependence of the PSNR on the h smoothing parameter for the LENA test image contaminated by the noise model NM1. As can be observed, the optimal value of the smoothing parameter h, for which the PSNR measure attains the maximal value depends significantly on the contamination level p, defined as the percentage of corrupted pixels. Figure 6 depicts the dependence of the mean values of r_c, r_m and r_d denoted as $\hat{r}_c$, $\hat{r}_m$ and $\hat{r}_d$ on the contamination level p. As can be observed, the increase of the mean values of the r_d is linearly dependent on the noise level p, which enables to estimate the noise level knowing the mean value of $\hat{r}_d$ derived from its histogram. Figure 7 shows that the linear dependence of r_d is similar for the commonly used test images (Fig. 1).

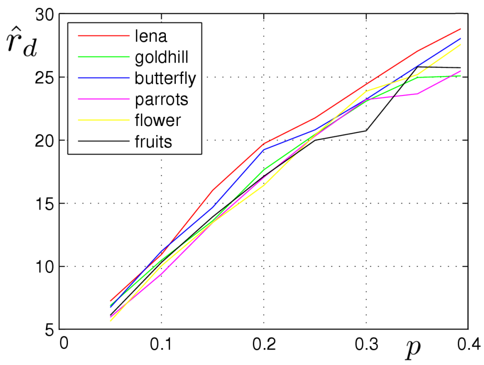

Fig. 7. Dependence of $\hat{r}_d$ on the noise intensity p .

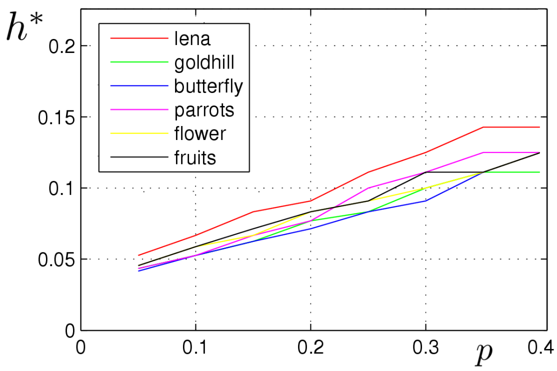

Fig. 8. Dependence of the optimal parameter h^* on the noise intensity p.

Figure 8 exhibits the dependence of the optimal value of the inverse of the optimal smoothing parameter, which will be denoted as $h^* = 1/h$ on the noise intensity p . This dependence is also of linear character, which enables to combine the values of $\hat{r}_d$ and h^* as they are both linearly dependent on the noise intensity. For the experiments 9 test images depicted in Fig. 1 and distorted by 3 noise model were used. The experimentally found formula, allowing to estimate the optimal normalization parameter h is then, (Fig. 9):

$$h^* = 0.00398 \cdot \hat{r}_d + 0.0177, \quad h^* = 1/h. \tag{6}$$

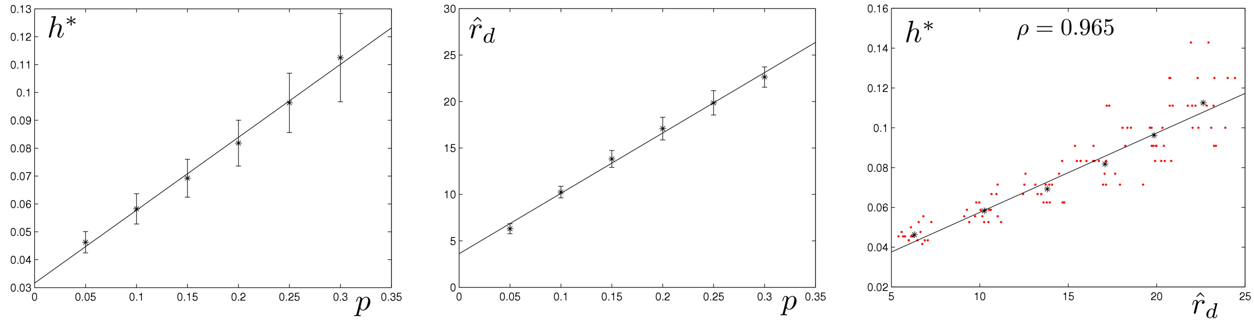

(a) (b) (c)

Fig. 9. Dependence between the optimal smoothing parameter h^* and the mean value $\hat{r}_d$: (a) linear dependence betweeen h^* and noise intensity p , (b) linear dependence between $\hat{r}_d$ and p , (c) linear dependence between h^* and p . In the plots (a) and (b) the standard deviations are shown and in plot (c) all data points delivered by the evaluation of 9 test images (Fig. 1) contaminated by three noise types of various intensities are depicted.

The effectiveness of the proposed filtering design was compared with a set of the most efficient noise removal switching filters evaluated in the extensive survey [8]: *Adaptive Center-Weighted Directional Distance Filter*, (ACWDDF), *Peer Group Filter*, (PGF), *Sigma Directional Distance Filter based on Rank*, (SDDFr), *Adaptive Center-Weighted Vector Median Filter*, (ACWVMF), *Adaptive Center-Weighted Vector Directional Filter*, (ACWVDF), *Modified Center-Weighted Vector Median Filter*, (MCWVMF), *Sigma Directional Distance Filter based on Mean*, (SDDFm), *Sigma Vector Median Filter based on Rank*, (SVMFr) and *Fast Fuzzy Noise Reduction Filter*, (FFNRF).

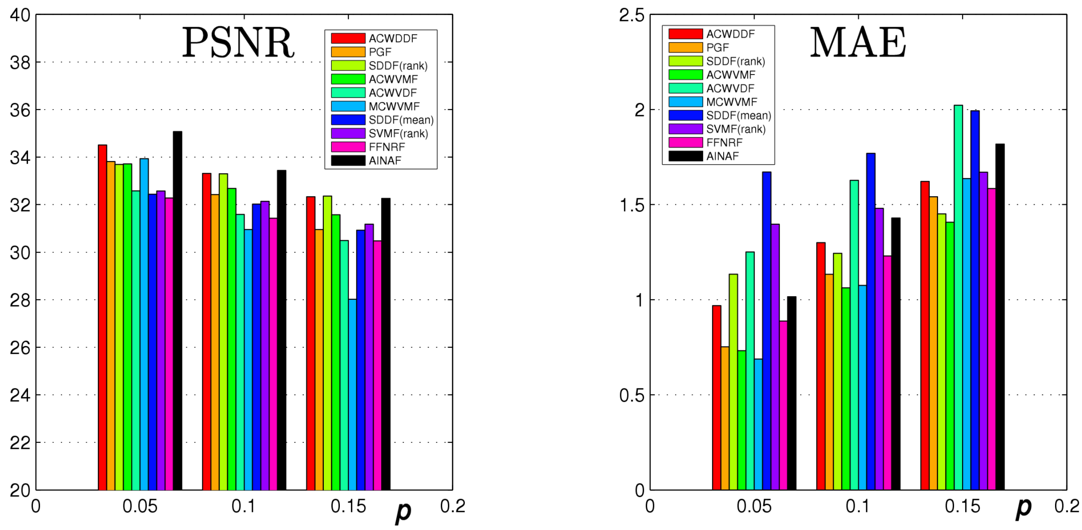

Fig. 10. Comparison of the proposed noise reduction technique in terms of PSNR and MAE with other denoising methods, (colour test image RAFTING contaminated by the uniform noise NM1).

Analyzing the plot presented in Fig. 10 which shows the filtering results obtained for the test color image RAFTING contaminated with uniform noise NM1 of intensity 0.05, 0.1 and 0.15, it is clear that the proposed filtering approach significantly outperforms in terms of the PSNR measure the most efficient filtering designs known in the literature [8]. The MAE measure is similar to the analyzed filters, which is due to the smoothing introduced by the VMF in the applied weighting scheme of the proposed filter. The excellent behavior of the new filter is also confirmed in Tab. 1 which summarizes the results obtained for the RAFTING, LOCOMOTIVE and MOTORBIKES test images. The subjective analysis of the filtering results offered by the new filter and the methods used for comparisons is provided in Fig. 11, which shows the restored cDNA image. As can be observed the new technique removes the impulses injected by the noise process and preserves the fine image details.

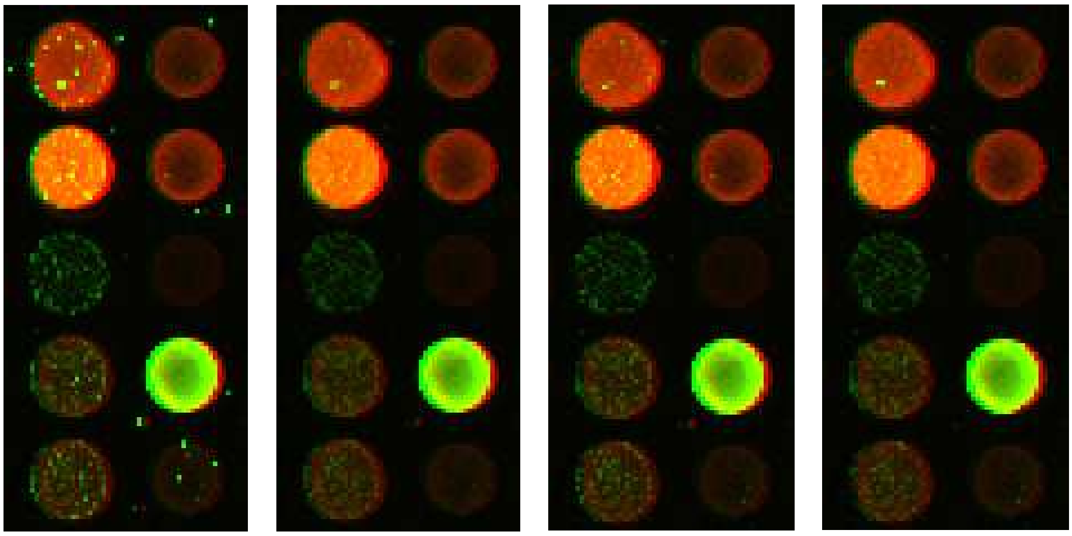

cDNA image | proposed filter output | ACWDDF output | PGF output

Fig. 11. Comparison of the efficiency of the proposed filter with the SANRFand FANRF noise removal techniques when restoring a noisy cDNA image

Table 1. Comparison of the filtering efficiency of the proposed filter as compared with the best filters evaluated in [8] for the RAFTING, LOCOMOTIVE and MOTORBIKES test images contaminated by the uniform noise NM1 with p=0.1

IMAGE	RAFTING		LOCOMOTIVE		MOTORBIKES	
FILTER	MAE	PSNR	MAE	PSNR	MAE	PSNR
PROPOSED	1.43	33.44	4.05	25.64	1.79	31.49
ACWDDF	1.30	33.31	2.94	26.55	1.62	31.64
PGF	1.13	32.42	4.16	24.58	1.60	30.29
SDDFr	1.24	33.30	2.82	26.63	1.33	32.17
ACWVMF	1.06	32.68	3.71	24.71	1.48	30.29
ACWVDF	1.63	31.59	3.35	25.62	2.14	29.28
MCWVMF	1.08	30.95	2.01	25.99	1.19	29.08
SDDFm	1.77	32.02	3.67	25.82	1.99	30.51
SVMFr	1.48	32.14	3.54	25.21	1.61	30.28
FFNRF	1.23	31.43	4.61	23.09	1.68	29.15

5. CONCLUSIONS

In the paper an adaptive filtering design for impulsive noise removal is proposed. The proposed noise detector together with the adaptive scheme of choosing the optimal value of the weighting parameter used in the construction of the filter exhibits very good denoising properties outperforming the known filtering solutions. The simplicity of the new algorithm and its computational speed makes the noise removal method very useful in the preprocessing of color images corrupted by impulse noise.

BIBLIOGRAPHY

[1] PLATANIOTIS K.N., VENETSANOPOULOS A.N., *Color Image Processing and Application,* Springer Verlag, August 2000.

[2] ASTOLA J., HAAVISTO P., NEUVO Y., Vector median filters. Proc. of the IEEE, vol. 78, no. 4, pp. 678-689, 1990.

[3] LUKAC R., SMOLKA B., MARTIN K., PLATANIOTIS K.N., VENETSANOPOULOS A.N., Vector filtering for color imaging. *IEEE Signal Processing Magazine*, Special Issue on Color Image Processing, Vol. 22, No. 1, pp. 74-86, 2005.

[4] SMOLKA B., PLATANIOTIS K.N., VENETSANOPOULOS A.N., Nonlinear techniques for color image processing, in *Nonlinear Signal and Image Processing: Theory, Methods, and Applications*, pp. 445-505, CRC Press, 2004.

[5] SMOLKA B., VENETSANOPOULOS A.N., Noise reduction and edge detection in color images, in *Color Image Processing: Methods and Applications*, pp. 75-100, CRC Press, 2006.

[6] LEE J.S., Digital image enhancement and noise filtering by use of local statistics. IEEE Trans. on PAMI, Vol. 2, No. 2, 165-168, 1980.

[7] KUAN D.T., SAWCHUK A.A., STRAND T.C., CHAVEL P., Adaptive noise smoothing filter for images with signal-dependent noise. IEEE Trans on PAMI, Vol. 7, No. 2, pp. 165-177, 1985.

[8] CELEBI M.E, KINGRAVI H.A., ASLANDOGAN Y.A., Nonlinear vector filtering for impulsive noise removal from color images, Journal of Electronic Imaging, Vol. 16, No. 3, 2007, pp. 033008.